ELSEVIER

Thermochimica Acta 245 (1994) 89–119

thermochimica acta

Relative stabilities of biomolecules at high temperatures and pressures ☆

Harold C. Helgeson *, Jan P. Amend

Department of Geology and Geophysics, University of California, Berkeley, CA 94720, USA

Abstract

Determination of the thermodynamic properties of biomolecules at elevated temperatures and pressures is critical to understanding enzymatic activity and the role of hyperthermobarophilic microbes in both industrial and natural hydrothermal processes. Experimental data reported in the literature indicate that amino acids and other aqueous biomolecules become increasingly sensitive to their chemical environment with increasing temperature. If this environment is not conducive to metastable preservation of biomolecules, they become highly reactive at high temperatures and pressures. However, increasing temperature does not then simply result in decomposition of biomolecules to form H_2O, CO_2, H_2, and/or other "inorganic" species, but instead they react to form additional "organic" and/or "inorganic" molecules, which may or may not achieve metastable equilibrium with one another under the conditions prevailing in the system. These conditions include the chemical potentials of H_2 (and therefore O_2) [1], CO_2, NH_3, and H_2S. If the chemical potentials of these components are favorable, amino acids and other bimolecules may persist at high temperatures for periods of time well in excess of those required for regeneration of the molecules, either abiotically or by hyperthermobarophilic microbes. Because irreversible reaction of biomolecules with other aqueous species, as well as metastable equilibrium states resulting from such reactions are highly sensitive to the activities of H_2, CO_2, NH_3, H_2S, and

☆ Plenary lecture presented at the Czechoslovak–French–Polish Conference on Calorimetry and Experimental Thermodynamics: Applications to Contemporary Problems, Prague, Czech Republic, 4–7 September 1993.

* Corresponding author.

[1] The chemical potentials of H_2 and O_2 (μ_{H_2} and μ_{O_2}, respectively) are related to each other at equilibrium by $\mu_{O_2} = 2(\mu_{H_2O} - \mu_{H_2})$, where μ_{H_2O} stands for the chemical potential of H_2O in the system. Hence, the activity a_{O_2} of O_2 in the aqueous phase can be expressed in terms of the corresponding activities a_{H_2} of H_2 and a_{H_2O} of H_2O by writing $a_{O_2} = (a_{H_2O}K/a_{H_2})^2$, which corresponds to the law of mass action for the reaction $H_2O \rightleftharpoons 0.5O_2 + H_2$. For dilute aqueous solutions, $a_{H_2O} \approx 1$ and $\mu_{H_2O} \approx \mu^\circ_{H_2O}$. Under these conditions, the first two equations in this footnote reduce to $\mu_{O_2} = \mu^\circ_{H_2O} - \mu_{H_2}$ and $a_{O_2} = (K/a_{H_2})^2$.

SSDI 0040-6031(94)01848-B

other species in solution, these activities must be controlled or at least monitored to achieve unambiguous results in hydrothermal experiments designed to measure the thermodynamic properties of biomolecules as a function of temperature and/or pressure. Such experiments are necessary to calibrate and verify equations of state, which can then be used to characterize the thermodynamic behavior of biomolecules at elevated temperatures and pressures. Only by quantifying this behavior can we determine optimal conditions for enzymatic activity and predict the degree to which reactions among amino acids, polypeptides, proteins, nucleic acids, and other aqueous species are exergonic at high temperatures and pressures. Carefully controlled hydrothermal studies of enzymes and other biomolecules produced by hyperthermobarophilic microbes as a function of temperature, pressure, and the chemical potentials of H_2, CO_2, NH_3, H_2S, and other components of the system should lead to development of new avenues of medical research and a better understanding of bacterial genetics, enzymatic catalysis, DNA replication, and many other biochemical processes on which life depends.

Keywords: Biomolecules; High pressure; High temperature; Hydrogen fugacity; Hyperthermobarophilic microbe; Stability; Thermodynamics

1. Introduction

Aqueous biomolecules have been both abiotically synthesized from, and degraded to "organic" and "inorganic" species at high temperatures many times in dozens of laboratories over the past 40 years or so, including some at temperatures as high or higher than those encountered in submarine hot springs [1,2]. Over the same period, considerable evidence has accumulated indicating that organic molecules may persist and/or be formed from both "organic" and "inorganic" precursors at high temperatures and pressures in the Earth [3–7]. These observations indicate that the formal distinction between organic and inorganic chemistry decreases dramatically with increasing temperature and pressure. It is also clear from the experimental data that have accumulated over the years that amino acids and other biomolecules become highly responsive to their chemical environment at elevated temperatures. Hence, it seems likely that the side chains of peptides, polypeptides, and proteins, as well as nucleic acid bases also become increasingly sensitive to their chemical environment with increasing temperature and pressure.

The upper temperature/pressure limits of protein folding and DNA melting have yet to be determined definitively for all but a few biomolecules, none of which are characteristic of hyperthermobarophilic archaea or bacteria. Furthermore, the extent to which protein folding, enzyme activity, and DNA melting depend on the chemical potentials of H_2, CO_2, NH_3, and H_2S has not been established unambiguously for any of these molecules at any temperature and pressure. Nevertheless, the chemical potentials of H_2, CO_2, NH_3, and H_2S in living systems vary widely from those in the human body to the chemical potentials of these species in oceanic hot springs where large colonies of diverse life occur at elevated temperatures and pressures [8–12] and those at depth in the Earth where hyperthermobarophilic

chemolithoautotrophs are thriving [13]. Depending on the chemical potentials of H_2 and CO_2 in the system and the extent to which it is open, some of these microbes may be surviving on both energy and nutrients produced by the irreversible disproportionation of the light paraffins in petroleum at the oil–water interface in hydrocarbon reservoirs [7]. Because hydrolytic oxidation/reduction reactions are generally favored at high temperatures, these reactions may lead in natural systems to metastable equilibrium states at elevated temperatures and pressures among biomolecules and other aqueous species that correspond to the distribution of species in solution with the lowest attainable Gibbs free energy over geologic time [5,7,14–16]. The extent to which these equilibrium states can be achieved in laboratory experiments depends in part on the chemistry of the system. The purpose of the present communication is to demonstrate that unambiguous experimental determination of the thermodynamic properties of biomolecules at high temperatures and pressures requires control of the chemical potentials of H_2, CO_2, NH_3, H_2S, and other aqueous species at optimal levels to promote metastability of the molecule under the conditions prevailing in the experiment. Equilibrium constants for chemical reactions among biomolecules and other aqueous species at high temperatures and pressures can then be computed with the aid of equations of state, which can be used in conjunction with other experiments to identify chemical environments that favor biomolecular stability and enzyme activity at elevated temperatures and pressures. This approach should greatly decrease the number of experiments which would otherwise be required to quantify the thermodynamic behavior of biomolecules at high temperatures and pressures.

Increasing biological and biochemical evidence indicates that thermophilic microbes flourish at temperatures as high as 100°C or more [17] and one experimental study that has never been reproduced [18] suggests that colonies of hyperthermobarophiles may persist at temperatures as high as 250°C in submarine hot springs. Experimental data also indicate that some hyperthermophiles are either barophilic or barotolerant at pressures as high as 750–880 bar at temperatures ranging up to 90°C or more [19,20]. Furthermore, biomolecules derived from hyperthermobarophilic microbes have been shown to persist in vitro at temperatures in excess of 140°C [12,21,22] and pressures as high as 1700 atm at temperatures above 100°C [23]. In fact, increasing temperature and pressure generally increases the activities of enzymes derived from thermobarophiles [12,22,24], yet the thermodynamic properties of relatively few of these molecules are known at elevated temperatures and pressures. The practical value of understanding the thermodynamic behavior of biomolecules as a function of temperature and pressure is underscored by the fact that many of the enzymes used in biotechnology, including those used in genetic engineering to replicate DNA in vitro are derived from thermophiles [22,25], yet both high-temperature enzymes and thermophilic microbes are nevertheless rarely studied calorimetrically. The DNA polymerase most widely used for this purpose is derived from *Thermus aquaticus*. Although this organism has an optimal growth temperature of about 70°C at approximately 1 bar [26], an even more efficient DNA replicating enzyme has been extracted from the hyperthermophile *Pyrococcus furiosus* [27], which has an optimal growth temperature of about 100°C at approximately 3 bar [28].

Experimental determination over the past decade of rates of amino acid degradation in unfavorable chemical environments at elevated temperatures and pressures by White [29], Bernhardt et al. [30], and others has led to the widely held perception that life is probably not possible at temperatures approaching about 150°C [13,17]. However amino acids have recently been synthesized at 150°C, where under favorable conditions they have been shown to persist at appreciable concentrations for more than 2 days [31]. Amino acids have also recently been synthesized and demonstrated to persist under favorable conditions for at least 2 h at much higher temperatures, from 200 to 275°C [32]. Because all biochemical degradation and synthesis experiments are of necessity carried out in vitro, their significance with respect to temperature and pressure limits of life depend on the extent to which they represent in vivo processes in organisms, some of which may lead to relatively high intracellular concentrations of specific aqueous species that contribute to the thermal stability of the organism [12,33,34]. In this context, experimental rates of biochemical degradation are indicative of temperature and pressure limits of life only to the degree to which intracellular chemistry was replicated in the in vitro experiments, and the extent to which the measured degradation rates of biomolecules such as amino acids, polypeptides, and nucleic acids exceed regeneration rates in living organisms. The absence of regenerative enzymes in such experiments would seem to be a fatal flaw in relating the results of the experiments to life at high temperatures and pressures! In any event, the possible relevance of the half-lives of biomolecules in hydrothermal experiments to the persistence of life at high temperatures can be assessed indirectly by comparing the results of the experiments with minimum regeneration rates of biomolecules in hyperthermobarophilic microbes. These rates correspond to minimal doubling times for the microbes at high temperatures and pressures.

2. Doubling times of hyperthermobarophilic microbes as a function of temperature and pressure

Doubling times at about 3 bar of *Methanopyrus kandleri* (AV19) reported by Huber et al. [35] and Kurr et al. [36] are shown as a function of temperature in Fig. 1, where it can be seen that the doubling time of this methanogen decreased dramatically with increasing temperature from 20 h at 85°C to about 1 h at an optimal growth temperature of approximately 96°C. Doubling times of *Pyrococcus furiosus* at about 3 bar given by Fiala and Stetter [37] are shown in Fig. 2 as a function of temperature, and in Fig. 3 as a function of pH and NaCl concentration at 100°C. It can be deduced from the curve in Fig. 2 that increasing temperature from about 70 to 100°C decreases the doubling time of *Pyrococcus furiosus* by almost an order of magnitude from about 275 min to about 37 min at the optimal growth temperature of approximately 100°C. Further increase in temperature caused the doubling time to increase. Similarly, it can be seen in Fig. 3 that increasing pH or NaCl concentration at 100°C from 5 or 0.1 wt%, respectively, dramatically decreases the approximate doubling time from 102 and 145 min to

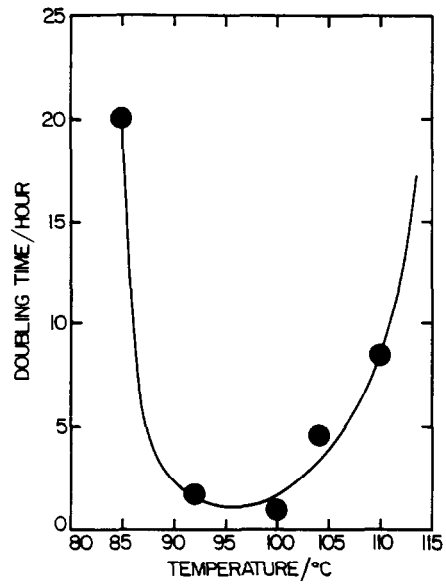

Fig. 1. Doubling time of *Methanopyrus kandleri* (AV19) in anaerobic sterile mineral medium [113] containing 1.5% NaCl in the presence of an H_2–CO_2 atmosphere as a function of temperature at about 3 bar reported by Huber et al. [35] and Kurr et al. [36].

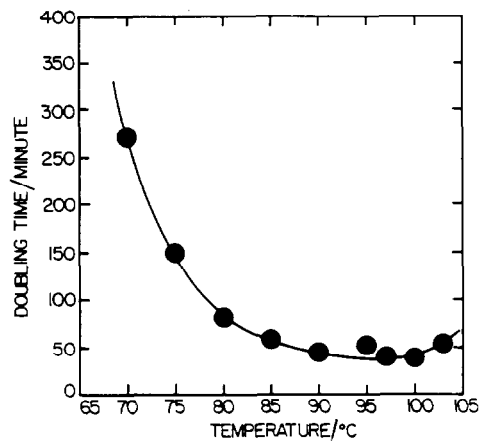

Fig. 2. Doubling time of *Pyrococcus furiosus* in "SME" medium [114] containing yeast extract, peptone, tryptone, meat extract, and other nutrients in the presence of sulfur reported by Fiala and Stetter [37] as a function of temperature at about 3 bar.

37 min at the optimal pH and NaCl concentrations of 7.5 and 0.32–0.59 wt%, respectively. Further increase in pH and NaCl concentrations caused the doubling time to increase.

Doubling times computed from specific growth rates reported by Jones et al. [38] for *Methanococcus jannaschii* at about 1 bar and Pledger and Baross [39] for ES4

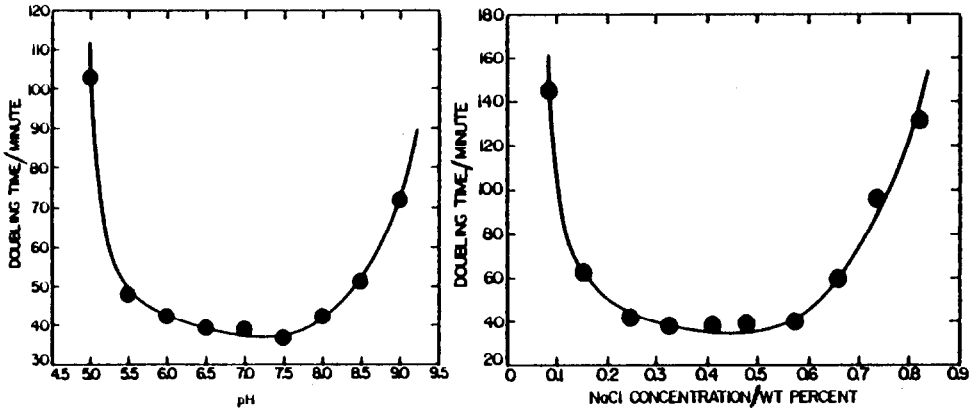

Fig. 3. Doubling time of *Pyrococcus furiosus* in "SME" medium [114] at about 3 bar and 110°C as a function of pH and NaCl concentration reported by Fiala and Stetter [37]; see caption to Fig. 2.

at about 2 bar are plotted against temperature in Fig. 4, where it can be seen that the approximate doubling time of *Methanococcus jannaschii* decreased from 275 min at 51°C to 27 min at the maximum growth temperature of 86°C. Jones et al. [38] report no growth at 100°C, which is the only constraint on the dashed extrapolation shown in Fig. 4. In contrast, the doubling time of ES4 decreased to a minimum of about 60 min at approximately 88°C and growth ceased at about 110°C.

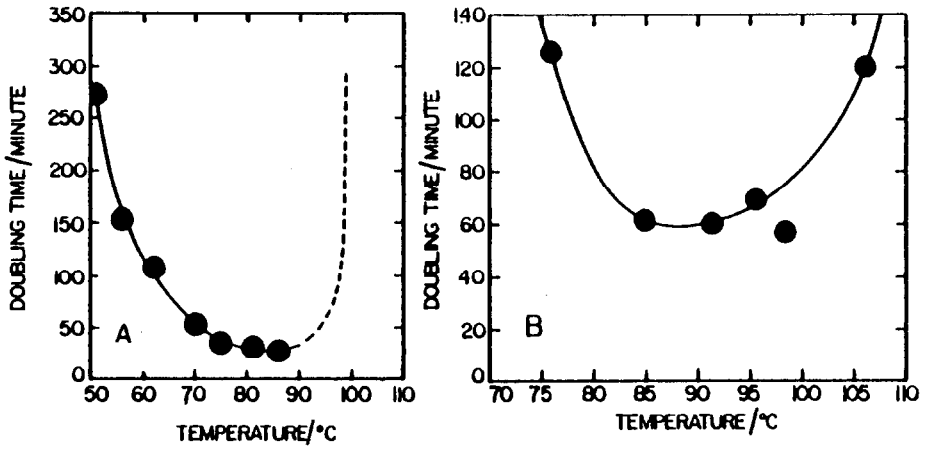

Fig. 4. Doubling times of (A) *Methanococcus jannaschii* in a defined growth medium consisting of an approximately 0.5 *m* NaCl solution containing K_2HPO_4, $CaCl_2$, NH_4Cl, $MgSO_4$, $MgCl_2$, KCl, $NiCl_2$, $NaSeO_4$, $NaHCO_3$, cysteine, Na_2S, $Fe(NH_4)_2(SO_4)_2$, vitamins, yeast extract, and other nutrients and (B) ES4 in artificial sea water containing yeast extract, vitamins, amino acids, peptone and other nutrients in the presence of elemental sulfur, as a function of temperature at about 1 and about 2 bar computed from growth rates reported by Jones et al. [38] and Pledger and Baross [39], respectively.

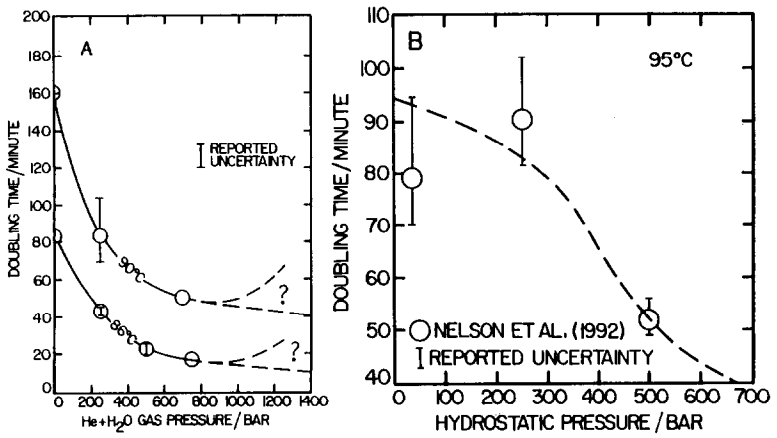

Fig. 5. Doubling times of (A) *Methanococcus jannaschii* at 90 and 95°C in the medium used in the growth experiments for the microbe described in the caption of Fig. 4, (B) ES4 at 95°C in artificial sea water in the presence of sulfur, as a function of pressure computed from growth rates reported by Miller et al. [41,71], Clark and Kelley [19], Clark [115], and Nelson et al. [42].

The pressure dependence of the doubling times of *Methanococcus jannaschii* at 86 and 90°C is shown in Fig. 5, together with that of ES4 at 95°C. It can be deduced from this figure that increasing pressure decreased dramatically the experimental doubling times of these organisms. The same behavior is exhibited by other hyperthermobarophiles, including *Pyrococcus abyssi* [40]. Note in Fig. 5 that *Methanococcus jannaschii* reached a doubling time of only 17 min at 86°C and 750 bar. The minimum doubling-time pressure for this microbe has yet to be established. Two possible extrapolations to pressures above 750 bar are shown in Fig. 5 for each of the *Methanococcus jannaschii* isotherms. Although no experimental data are available to adequately control extrapolation of low-temperature/pressure rates of in vivo protein synthesis and DNA replication to high temperatures and pressures, the dashed extrapolations of the doubling time curves for *Methanococcus jannaschii* in Fig. 5 afford at least an estimate of possible minimum regeneration rates for these molecules in *Methanococcus jannaschii* at high temperatures and pressures in excess of 750 bar.

The doubling-time curves shown in Figs. 1–4 are representative of those of many other thermophilic archaea and bacteria that have been studied experimentally. Growth rates for about 50 such microbes representing about 20 different genera have now been documented in the laboratory as a function of temperature and in many instances pH and NaCl concentration [12,17,22,28]. Although some experimental information has been reported for different oxidation states of sulfur in mineral substrates used in these experiments, no comprehensive studies of the dependence of hyperthermobarophilic growth rate on the chemical potentials of H_2, CO_2, NH_3, and H_2S have been carried out. The media, substrates, nutrients, carbon and energy sources, and the type of experimental apparatus used in the various thermophilic microbial growth-rate studies reported in the literature vary

widely from study to study, which may have had a substantial effect on the relative doubling times of the various thermophiles that have been investigated. Some of these differences can be assessed in the captions of Figs. 1–4. For example, the large discrepancy in Figs. 4 and 5 between the low-pressure doubling times computed from growth rates of *Methanococcus jannaschii* at 86°C measured by Miller et al. [41] and those reported by Jones et al. [38] for this microbe at 86°C and 1 bar can probably be attributed to the fact that Miller et al. [41] used stainless steel containers, but glass incubators were used in the latter study. At low pressures, stainless steel apparently inhibits microbial growth, but this inhibition is overcome with increasing pressure.

A number of factors may account for the low-pressure discrepancy in Figs. 4 and 5 between the doubling times of ES4 computed from growth rates reported by Pledger and Baross [39] at about 2 bar and those generated from growth rates given by Nelson et al. [42]. For example, Pledger and Baross [39] used glass tubes and a complex organic medium containing proteins and yeast extract to promote growth. Nelson et al. [42] used gold-lined vessels and different media. Comparisons of this kind among various hyperthermobarophilic microbial growth-rate experiments leave little doubt that the results of such studies strongly depend on the chemical and physical characteristics of the experiments. Consequently, they are not necessarily indicative of maximal growth rates that could be achieved in either nature or the laboratory by the same organism at its optimal growth temperature and pressure under different chemical and/or physical conditions. It is of interest to note in this regard that no attempt has been made in any of the experimental growth studies of hyperthermobarophilic microbes that have so far been carried out to duplicate the chemical and mineralogic environment in which the microbes thrive in nature. Nevertheless, there is no doubt from these studies that under favorable laboratory conditions, hyperbarothermophiles can exist at temperatures in excess of 110°C and pressures to at least 880 bar.

Although the upper temperature limit of microbial life at high pressures has yet to be determined, it is clear from growth-rate studies of hyperthermobarophilic microbes such as *Methanopyrus kandleri*, *Methanococcus jannaschii*, and ES4 represented by the curves shown in Figs. 1, 4, and 5 that the minimum regeneration times of enzymes and other biomolecules on which microbial life depends at high temperatures and pressures is a matter of minutes, not hours or days. It follows that experimental studies in which amino acids react to form other species at high temperatures and pressures have little relevance to the possible existence of hyperthermobarophilic life unless the time required for degradation of the amino acids is shorter than these regeneration times, which under the most favorable conditions may in some cases decrease to a matter of seconds as temperature and pressure increase beyond those at which microbial life has so far been shown to be possible.

3. Relative stabilities of amino acids at high temperatures and pressures

Experiments designed to assess the extent to which amino acids degrade at high temperatures and pressures have been carried out over the past decade by White [29],

Bernhardt et al. [30], Miller and Bada [43], Bada [44], Bada et al. [45,46], and others. For example, White [29] measured half-lives of a wide variety of aqueous biomolecules including amino acids, proteins, and nucleic acids in sealed glass tubes immersed in an oil bath at 250°C and concluded that hyperthermophilic life as we know it could not survive at this temperature, which contradicts Baross and Deming's [18] experimental finding that a community of hyperthermobarophilic microbes collected from submarine hot springs on the East Pacific Rise grew in their laboratory experiments at 250°C and 268 bar. Baross and Deming's [18] controversial experimental results were called into further question by Trent et al. [47], who claimed on the basis of their high temperature-pressure experiments with a non-thermophilic bacterium (*Vibrio harveyi*) that Baross and Deming's [18] results may not have been a consequence of microbial growth at 250°C and 268 bar, but may instead have been due to artifacts produced in the medium and contamination during sample processing. Baross and Deming [48] denied this possibility, citing among other things crucial differences between the two studies as well as differences in Baross and Deming's [18] experimental observations at 250 and 300°C. Unfortunately, the microbial cultures used by Baross and Deming [18] were not preserved and all efforts to replace them have failed [50].

In another attempt to refute Baross and Deming's [18] results, Bernhardt et al. [30] encapsulated natural amino acids, polyglycine, and cells of the thermophile *Pyrodictium occultum* in nickel tubes containing various aqueous media. The tubes were sealed under 4 bar of nitrogen pressure and then pressurized to 260 bar and heated at 250°C for 6 h, which resulted in decomposition of aspartic and glutamic acid, serine, threonine, cysteine, and tryptophan, as well as partial degradation of histidine, arginine, and phenylalanine. In the process, glycine, alanine and ammonia were produced. The extent to which amines, amides, carboxylic acids, or other species were generated in the experiments is not known. In other heating experiments carried out by Bernhardt et al. [30] with acid solutions after 6 h of incubation at 260 bar, cysteine, glutamic and aspartic acid, threonine, serine, tryptophan, isoleucine and methionine began to react to produce glycine, alanine, and ammonia at temperatures above about 120°C. However, in sodium phosphate solutions with a buffered pH at 25°C of 7, substantial degradation of amino acids occurred only at temperatures above about 150°C. Bernhardt et al. [30] computed half-lives for the amino acids in their experiments of approximately 50 min or less. Although no effort was made to control or monitor the fugacity of H_2 or CO_2 in their experiments, they concluded on the basis of their observations that degradation of amino acids at high temperatures and pressures is too rapid and extensive for life to persist above about 150°C.

The conclusion reached by Bernhardt et al. [30] that life cannot exist above about 150°C was echoed four years later by Miller and and Bada [43], who also carried out experiments to demonstrate that biomolecules are unstable at high temperatures and pressures. In their experiments, aqueous solutions containing initially equal concentrations of aspartic acid, serine, alanine, and leucine were sampled over a 6 h period at 150°C and 268 bar. Leucine, serine, and aspartic acid decomposed rapidly with half-lives of the order of 15–20 min, a few minutes, and less than 1 min,

respectively. Miller and Bada [43] used these observations to refute the hypothesis advanced by Corliss et al. [51] that life on Earth may have originated in submarine hot springs. However, Miller and Bada [43] made no attempt to create a favorable chemical environment in their experiments to promote amino acid stability, and they give no indication of the extent to which ammonia, amines, amides, or carboxylic acids were produced in their experiments. However, glycine, which was absent initially, was produced together with alanine during the experiment, which was carried out without controlling or monitoring the oxidation state of the system. Subsequently, Shock [16] demonstrated that metastable equilibrium among leucine, glycine, and alanine was approached in Miller and Bada's [43] experiments in accord with

$$4\text{Alanine} \rightleftharpoons \text{Leucine} + 3\text{Glycine} \tag{1}$$

which represents the disproportionation of alanine to glycine and leucine. As such, it corresponds to the sum of

$$3\text{Alanine} + 4.5O_2 \rightleftharpoons 3\ \text{Glycine} + 3CO_2 + 3H_2O \tag{1A}$$

and

$$\text{Alanine} + 3CO_2 + 3H_2O \rightleftharpoons \text{Leucine} + 4.5O_2 \tag{1B}$$

Assertions to the contrary notwithstanding [46], the metastable equilibrium state represented by reaction (1) depends on the fugacity of oxygen in the system to the extent required by reactions (1A) and (1B).

Following Shock's [16] publication, Bada [44] and Bada et al. [45,46] have repeatedly attempted to demonstrate experimentally that such metastable equilibrium states do not occur. For example, Bada et al. [45] report formation in another experiment of ethanamine at the expense of alanine after 24 h of reaction at 250°C and 268 bar. No detectable glycine, leucine, or any other amino acid apparently formed in the experiment, which was cited as evidence that metastable equilibrium was not approached. However, the curves shown in Fig. 6 indicate that this conclusion may not be warranted. Metastable equilibrium between alanine and ethanamine can be described in terms of

$$\text{Alanine} \rightleftharpoons \text{Ethanamine} + CO_2 \tag{2}$$

for which the logarithmic analog of the law of mass action can be written as

$$\log f_{CO_2} = \log K_{(2)} - \log(a_{\text{Ethanamine}}/a_{\text{Alanine}}) \tag{3}$$

where f_{CO_2} stands for the fugacity of CO_2, $K_{(2)}$ refers to the equilibrium constant for reaction (2), and $a_{\text{Ethanamine}}$ and a_{Alanine} stand for the activities of the subscripted species in solution. Although Bada et al. [45] do not report CO_2 as a reaction product, the range of possible CO_2 fugacities that could have resulted from the decarboxylation of alanine in their experiments at 250°C is represented by the vertical arrow shown in the figure, which falls below the curve representing metastable equilibrium for a 100:1 ratio in solution of the activity of ethanamine to that of alamine. To achieve a ratio greater than this in their experiment would require more than 99% decomposition of alanine. As indicated above, Bada et al. [45] report 97% decomposition after 24 h of reaction.

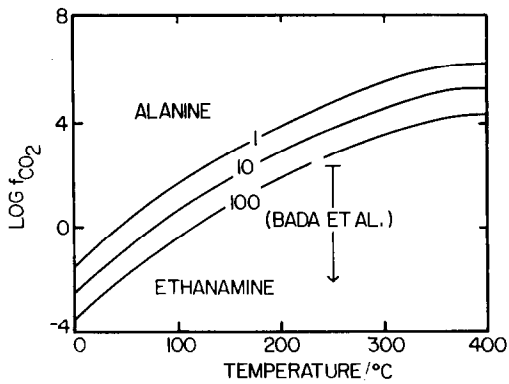

Fig. 6. Logarithm of the fugacity of CO_2 (f_{CO_2}) as a function of temperature at 268 bar representing metastable equilibrium between ethanamine and alanine for activity (a) ratios of ethanamine to alanine of 1, 10, and 100 computed from Eq. (3) using values of log K generated from $\log K = -\Delta\bar{G}_r^{\circ}/2.303RT$ and standard partial molal Gibbs free energies of reaction ($\Delta\bar{G}_r^{\circ}$) calculated with the aid of SUPCRT92 [82] using the equations of state given in Appendix A and parameters and thermodynamic data taken from Shock and Helgeson [86]. The possible range of CO_2 fugacities that may have obtained in the experiments carried out by Bada et al. [45] is represented by the vertical arrow. The maximal limit of these fugacities (about 190 bar) was computed from $f_{CO_2} = X_{CO_2}\chi_{CO_2}P$, where X_{CO_2} and χ_{CO_2} stand for the mole fraction and fugacity coefficient of CO_2, using phase equilibrium data taken from Bowers and Helgeson [56] and equations of state given by Belonoshko et al. [57].

In another attempt to discredit Shock's [16] calculations indicating that under favorable conditions metastable equilibrium states may be attained among amino acids and other aqueous species at high temperatures, Bada et al. [46] carried out experiments in which they heated aqueous phosphate solutions containing ethanamine and either L-alanine or glycine and D/L-leucine in glass tubes. A mixture of minerals consisting of quartz (SiO_2), fayalite (Fe_2SiO_4), and magnetite (Fe_3O_4) was added to a duplicate set of samples in an effort to determine possible effects of buffering the oxygen and hydrogen fugacities (f_{O_2} and f_{H_2}, respectively) in accord with

$$3SiO_2 + 2Fe_3O_4 \rightleftharpoons 3Fe_2SiO_4 + O_2 \tag{4}$$

and

$$H_2O \rightleftharpoons H_2 + 0.5O_2 \tag{5}$$

Because quartz, fayalite and magnetite are considered in the present context to be stoichiometric and the aqueous phase is relatively dilute, it follows from the standard state of unit activity of the pure component at any temperature and pressure that $a_{SiO_2} = a_{Fe_2SiO_4} = a_{Fe_3O_4} = 1 \approx a_{H_2O}$. Accordingly, the logarithmic analogs of the law of mass action for reactions (4) and (5) can be written as

$$\log f_{O_2} = \log K_{(4)} \tag{6}$$

and

$$\log f_{H_2} = \log K_{(5)} - 0.5 \log K_{(4)} \tag{7}$$

respectively, where $K_{(4)}$ and $K_{(5)}$ denote the equilibrium constants for the subscripted reactions at the temperature and pressure of interest. The glass tubes were degassed, sealed in a vacuum, and then encased in water-filled teflon-lined tubes, which were subsequently sealed with steel caps. They heated the samples at 240°C for up to 25 h and found that all three amino acids decomposed to form amines. No other reaction products were detected. Furthermore, they report that the decomposition of alanine to ethanamine was not affected by the presence or absence of the buffer represented by reaction (4), nor should it be (see reaction (2) above). No information is given by Bada et al. [46] concerning the effect of this buffer, or lack thereof on the decomposition of leucine or glycine in their experiments. In fact, it has been demonstrated experimentally elsewhere that quartz, fayalite, and magnetite cannot achieve equilibrium in accord with reaction (4) over laboratory timescales at temperatures below about 500°C [52]. However, these minerals almost certainly dissolved to some extent in the aqueous phase (perhaps incongruently in the case of fayalite), which may have appreciably affected the chemistry and pH of the solution. Despite such ambiguities, Bada [44] and Bada et al. [46] concluded from the results of their experiments that metastable equilibrium states cannot be achieved under any circumstances among organic aqueous species at high temperatures, especially those prevailing in submarine hot springs. It should perhaps be emphasized in this regard that Bada [44] and Bada et al. [46] made this sweeping generalization in spite of the fact that they failed to include an *effective* oxygen fugacity buffer and a favorable chemical environment in their experiments that would inhibit amino acid decomposition and promote metastable equilibrium states at high temperatures and pressures. Perhaps the clearest indication that such generalizations are unwarranted is provided by the results of the experiments carried out by Yanagawa and Kobayashi [53], who synthesized a variety of amino acids after 1.5 to 12 h at 325°C from methane and nitrogen in a modified submarine hydrothermal vent medium. They also demonstrated that peptide-like polymers can form in hydrothermal solutions at temperatures ranging from 250 to 350°C.

The results of the degradation experiments summarized in the preceding paragraphs contrast sharply with those of recent amino acid synthesis experiments, which clearly indicate that under favorable conditions, amino acids may form and persist at high temperatures over far greater time periods than the probable doubling times of hyperthermobarophilic microbes. For example, Hennet et al. [31] recently synthesized abiotically β-alanine and a wide variety of D- and L-α-amino acids from aqueous KCN, NH_4Cl, HCHO, and CH_3OH in the presence of a CO_2–H_2–H_2O gas mixture with a mole ratio of CO_2 to H_2 of about 3:1 using platinum powder and either NaHS and the mineral assemblage pyrite (FeS_2) + pyrrhotite (FeS) + magnetite (Fe_3O_4) in Experiment A or illite ($K_{0.8}Al_{1.9}(Al_{0.5}Si_{3.5})O_{10}(OH)_2$) in Experiment B. Both experiments were carried out in TiO_2-lined reactors at 150°C and 10 bar. Equilibrium among pyrite, pyrrhotite, and magnetite is consistent with

$$6FeS + 4H_2O \rightleftharpoons Fe_3O_4 + 3FeS_2 + 4H_2 \tag{8}$$

for which the law of mass action can be written for $a_{FeS} = a_{FeS_2} = a_{Fe_3O_4} = 1 \approx a_{H_2O}$

(see the text immediately preceding Eq. (6) above) as

$$f_{H_2} = K_{(8)} \tag{9}$$

where a_{FeS}, a_{FeS_2}, and $a_{Fe_3O_4}$ stand for the activities of the subscripted components of stoichiometric pyrrhotite, pyrite, and magnetite, a_{H_2O} designates the activity of H_2O in the aqueous phase, f_{H_2} refers to the fugacity of hydrogen in the system, and $K_{(8)}$ denotes the equilibrium constant for reaction (8).

It is not clear why Hennet et al. [31] included the minerals they did in their reaction vessels. The equilibrium state represented by reaction (8) almost certainly cannot be achieved experimentally over a time period of a few days at 150°C [54]. However, pyrite, pyrrhotite, magnetite, and illite would be expected to dissolve to some extent during the experiments, which would affect the chemistry of the aqueous phase. The hydrogen fugacity in the experimental system was probably buffered by the relatively large mole fraction of H_2 in the gas phase. Assuming equilibrium among CO_2, H_2O, H_2, and O_2 in Hennet et al.'s [31] experiments (which is somewhat problematical [55]) and taking account of phase relations in the system CO_2–H_2O [56], together with fugacity coefficients for H_2O, CO_2 and H_2 in the gas [57], it can be shown that the fugacity of H_2 in the experiments carried out by Hennet et al. [31] would have been about 2 bar.

Concentrations of some of the amino acids synthesized by Hennet et al. [31] are depicted in Figs. 7 and 8, where it can be deduced that the experiments produced

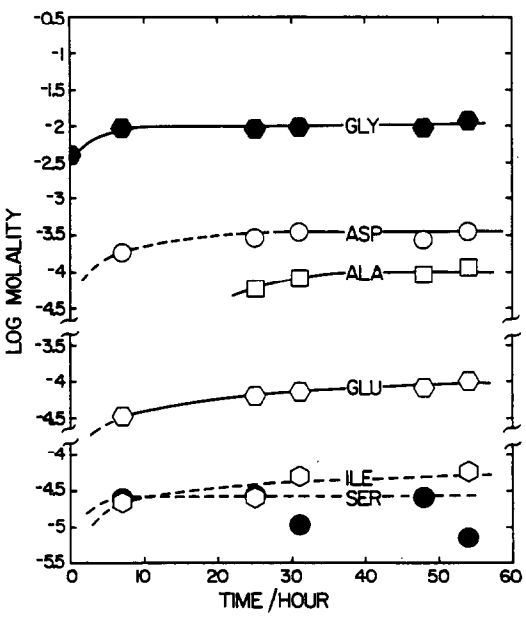

Fig. 7. Logarithms of the molalities of amino acids synthesized in Experiment A by Hennet et al. [31] at 150°C and 10 bar as a function of time (see text). The symbols correspond to those identified in Fig. 8.

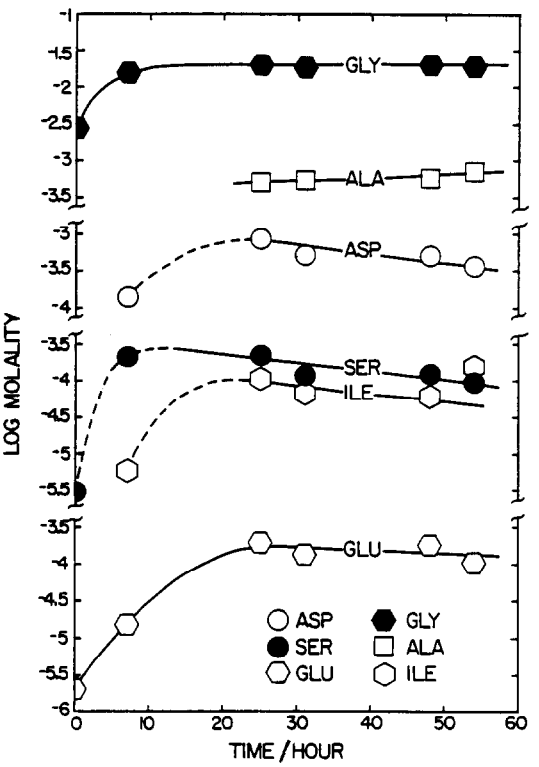

Fig. 8. Logarithms of the molalities of amino acids synthesized in Experiment B by Hennet et al. [31] at 150°C and 10 bar as a function of time (see text).

glycine, alanine, aspartic and glutamic acid, serine, and isoleucine. However, these amino acids were not generated with the same relative abundances in the two experiments. In Experiment A, the order of increasing concentration was serine, isoleucine, glutamic acid, alanine, aspartic acid, and glycine, but in Experiment B, the order was glutamic acid, isoleucine, serine, aspartic acid, alanine, glycine. Note that all of the curves shown in Fig. 7 are either flat or slightly positive in slope from about 10 to 54 h, with no indication of amino acid degradation, except possibly in the case of serine over the entire 54 h time period of the experiment. In contrast, the curves for all of the amino acids except glycine and alanine shown in Fig. 8 maximize and exhibit slightly negative slopes above about 25 h. However, the maximum decrease in amino acid concentrations from those corresponding to the extrema in Fig. 8 to those at 54 h is only about 30% or less over the 19 h time period. No increase or decrease in the concentration of glycine was documented beyond 25 h, but that of alanine increased slightly throughout Experiment B. The differences between the results of Experiments A and B reported by Hennet et al. [31] underscore the extreme sensitivity of aqueous amino acids to their chemical environment at elevated temperatures and pressures. In addition to the amino acids shown in Figs. 7 and 8, Hennet et al. [31] report tentative identification of traces of

lysine, histidine, and β-alanine formed in Experiment A, and traces of phenylalanine, histidine, and β-alanine in Experiment B. The chiralities of three of the amino acids (alanine, aspartic acid, and glutamic acid) synthesized in the experiments were determined and found to be racemic mixtures in all samples.

The experimental results reported by Hennet et al. [31], as well as those obtained nearly 25 years ago by Fox and Windsor [58] have been confirmed recently by Marshall [32], who synthesized amino acids from HCHO reacting separately with aqueous H_2 and/or H_2O_2 in NH_4HCO_3 or NH_4OH solutions containing in some instances NaCN and/or CH_3OH for 2 h at 110 and 210°C. Marshall [32] also synthesized amino acids by reacting for up to 2 h CaC_2 and Ca with aqueous NH_4HCO_3 solutions containing H_2O_2 at 225°C. In one 2 h experiment at 210°C, Marshall [32] synthesized glycine and traces of serine and aspartic acid from aqueous NH_4HCO_3 and H_2O_2, and in another he synthesized glycine, alanine, glutamic acid, and traces of serine, valine, and aspartic acid from aqueous NH_4OH, NaCN, and H_2.

Some of Marshall's [32] experimental results are depicted in Fig. 9, where it can be seen that the concentrations of glycine, alanine, aspartic acid, serine, leucine, isoleucine, and lysine synthesized in the experiments increased slightly from 110 to 210°C. The molality of proline was about the same at the two temperatures. Differences in the concentrations of amino acids synthesized by Marshall [32] in two experiments carried out for 0.2 and 2 h, respectively, can be assessed in Fig. 10. It can be seen in this figure that the concentrations at 225°C of glycine and alanine

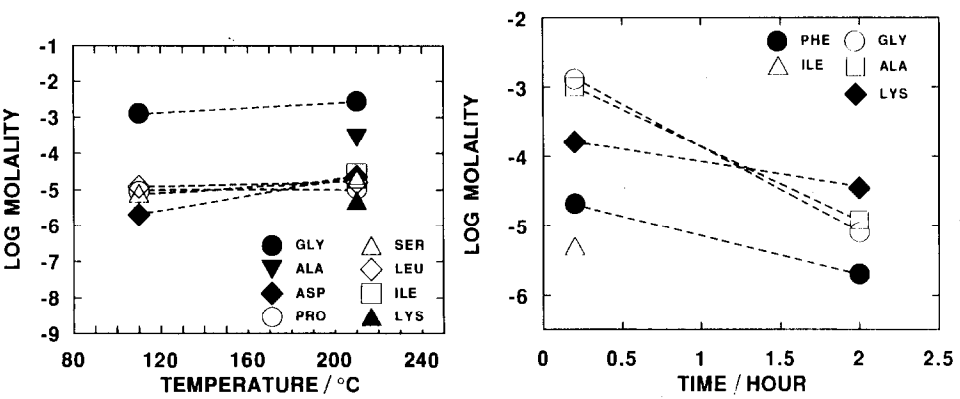

Fig. 9. Logarithms of the molalities of amino acids synthesized by Marshall [32] from HCHO, NH_4HCO_3, and H_2O_2 in aqueous solutions after 2 h at 110 and 210°C at P_{sat} (see below). The reactants at the two temperatures were identical but the partial pressure of oxygen and solution volume were 3 bar and 4 cm^3, respectively, in the 110°C experiment, and 17 bar and 10 cm^3 in the 210°C experiment. P_{sat} is used in the present communication to refer to pressures corresponding to liquid–vapor equilibrium for the system H_2O, except at temperatures lower than 100°C where it refers to the reference pressure (P_r) of 1 bar.

Fig. 10. Logarithms of the molalities of amino acids synthesized by Marshall [32] at 225°C and P_{sat} from Ca and CaC_2 reacting with aqueous solutions containing NH_4HCO_3 and H_2O_2 after 0.2 h and 2 h, respectively (see text and the caption to Fig. 9).

were lower after 2 h by about 2 log units and those of phenylalanine and lysine by about 1 log unit or less than the concentrations of these amino acids in the 0.2 h experiment. Nevertheless, the molalities of all four amino acids remained greater than 10^{-6}. The only difference in these two experiments was the partial pressure of H_2, which was 24 bar in the 0.2 h experiment and 20 bar in the 2 h experiment. In addition to the amino acids shown in Figs. 9 and 10, threonine was also synthesized by Marshall [32]. The fact that Marshall [32] synthesized both the same amino acid from different reactants and different amino acids from the same reactants in the presence or absence of H_2 and/or O_2 leaves little doubt that amino acids are sensitive to their chemical environment and the oxidation state of the system at high temperatures.

The experimental data and observations summarized in the preceding five paragraphs call into serious question the widely held notion shared by White [29], Bernhardt et al. [30], Miller and Bada [43], Bada [44], and Bada et al. [45,46] that under any circumstance aqueous amino acids are highly unstable and decompose rapidly at and above about 150°C with half-lives that are too short to support life at these temperatures. They also leave little doubt that amino acids are sensitive to their chemical environment and the oxidation state of the system at high temperatures. Under unfavorable conditions these aqueous molecules are highly reactive at high temperatures, but under favorable conditions they may be synthesized and/or persist at high temperatures and pressures for periods of time well in excess of the probable doubling times of hyperthermobarophilic microbes under these conditions. This observation supports the general significance of the abiotic hydrothermal synthesis of organic compounds reported 40 years ago by French [59], as well as the credibility of the hypothesis advanced by Ingmanson and Dowler [60] and Corliss et al. [51] that life on Earth may have originated in submarine hot springs. It also vindicates Baross and Deming's [18] experimental results and underscores the danger of using the results of experiments in which no effort is made to promote amino acid stability to discredit the possibility that under more favorable conditions these species may form and persist at high temperatures and pressures. To do so in the present state of knowledge is as much a non sequitur as the following quote by Ingle [61] from Lewis Carroll's Alice in Wonderland

> "Consider your verdict," the King said to the jury. "Not yet, not yet!" the rabbit hastily interrupted. "There's a great deal to come before that."

Strong temperature and compositional gradients exist in submarine hot springs which may cause multiple generations of reactions to occur among biochemical molecules and other aqueous species long before the molecules react to form amines. The major factors controlling the relative stabilities of amino acids and other biomolecules at high temperatures and pressures in such systems appear to be the chemical potentials of H_2, CO_2, NH_3, and by inference, H_2S. The extent to which the relative stabilities of amino acids and other biomolecules depend on these variables at high temperatures and pressures requires systematic and comprehensive experimental investigation. Experiments are also needed to investigate side chain interactions in proteins at high temperatures and pressures, which may stabilize enzymes and other proteins required for hyperthermobarophilic microbial life.

4. Side chain interactions in proteins at high temperatures and pressures

The widely held notion that all proteins unfold at temperatures below or near 100°C is based primarily on calorimetric data at elevated temperatures for denaturation of only about a dozen proteins [62–67], none of which were extracted from hyperthermobarophilic microbes. The heat capacities and volumes of only four of these proteins (ribonuclease A, myoglobin, cytochrome *c*, and lysozyme) have been measured both in their native and denatured state at temperatures as high as 125°C and 75°C, respectively [67–69]. It thus appears that many more calorimetric and densimetric studies will be required before valid generalizations can be made about the upper temperature–pressure limits of exocellular protein stability.

Recent experimental studies of enzymes extracted from hyperthermophiles indicate that some are capable of enzymatic activity at temperatures and pressures well in excess of those at which the hyperthermobarophilic microbes from which they were extracted have been shown to grow. For example, Schuliger et al. [21] recovered an amylolytic enzyme from the hyperthermophile ES4 that exhibits activity at temperatures as high as 140°C, with maximal activity at about 125°C. ES4 has a maximum growth temperature of 100°C at about 2 bar [39]. Similarly, Constantino et al. [70] have shown that the enzyme α-glucosidase extracted from the hyperthermophile *Pyrococcus furiosus* exhibits optimal activity at temperatures ranging from 105 to 115°C. *Pyrococcus furiosus* has a maximum growth temperature of 103°C at about 3 bar [37]. In another study, Miller et al. [71] demonstrated that the enzymatic activity of hydrogenase extracted from *Methanococcus jannaschii* was more than tripled by an increase in pressure from about 7.5 to 263 bar at its optimal growth temperature of 86°C. Subsequently, Hei and Clark [72] reported pressure enhancement at 90°C and 500 bar of the thermal stability of F_{420}-nonreactive hydrogenase extracted from both *Methanococcus jannaschii* and *Methanococcus igneus*. The first of these microbes was isolated from submarine hot springs at a depth corresponding to about 260 bar with a maximum growth temperature of 100°C at 1 bar [38]. The second was isolated from a vent system at a depth corresponding to a pressure of about 106 bar with a maximum growth temperature of 91°C at about 1 bar [73]. Hei and Clark [72] also demonstrated increased thermal stability at 110°C and 500 bar of the enzyme α-glucosidase extracted from *Pyrococcus furiosus*, which was isolated by Fiala and Stetter [37] from beach sediments on the island of Vulcano, Italy. As noted above, this hyperthermophile had a maximum growth temperature of 103°C in their experiments at about 3 bar. Hence, pressure enhancement of enzyme activity and thermal stability is not unique to enzymes isolated from high-pressure environments, nor is it characteristic of all enzymes [72]. Nevertheless, increasing temperature and pressure above 100°C and about 250 bar may enhance substantially the stabilities of certain proteins and promote enzymatic activity and life at temperatures and pressures well beyond those generally thought to be possible. This observation is consistent with Amend and Helgeson's [74] and Shock's [75,76] thermodynamic calculations, which

indicate that increasing temperature lowers the energy required for ATP formation and organic dehydration reactions, including the formation of peptides from amino acids.

It follows from the fact that amino acids become so sensitive to their chemical environment at elevated temperatures and pressures that increasing temperature and pressure should also promote side chain interaction in proteins, which may contribute substantially to stabilizing the folded state at high temperatures and pressures. These interactions fall into various groups, five of which are represented by the examples of possible side chain interactions in lysozyme shown in reactions (10)–(14). The numbers in parentheses below the reactant molecules in reactions (10)–(14) designate the amino acid sequence number in lysozyme and the heavy bars represent the peptide backbone in the protein. The amino acid designations on the left sides of reactions (10)–(14), as well as those of the interchain complexes on the right sides of the reactions refer to the side chains and analogous organic molecules sans end groups, respectively.

Dehydration (10)

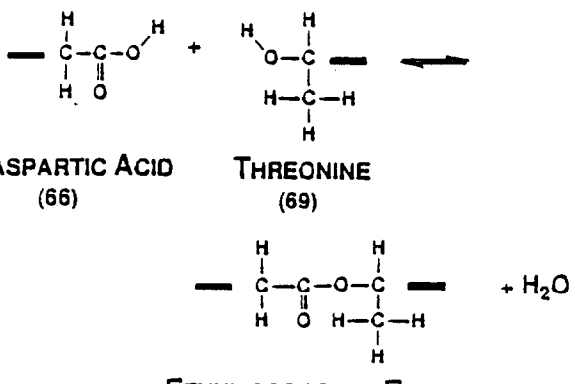

Oxidation (11)

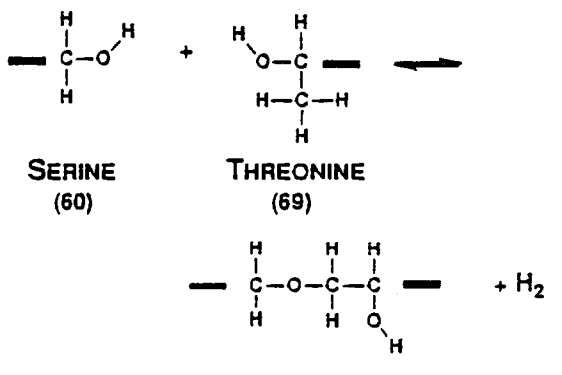

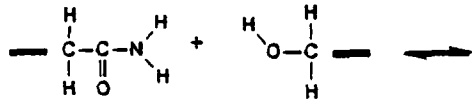

ASPARAGINE (65) SERINE (72)

Reduction (12)

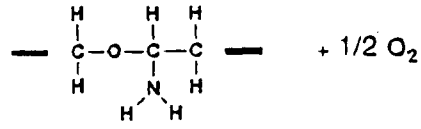

ETHYLAMINOPROPYL ETHER

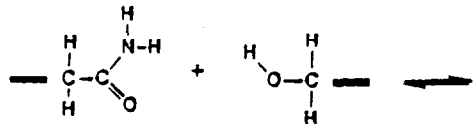

ASPARAGINE (59) SERINE (50)

Deaminization (13)

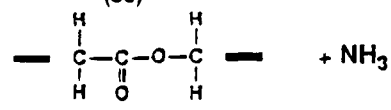

DIETHYL ESTER

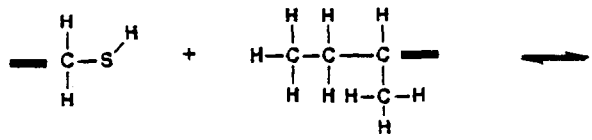

CYSTEINE (94) ISOLEUCINE (98)

Desulfurization (14)

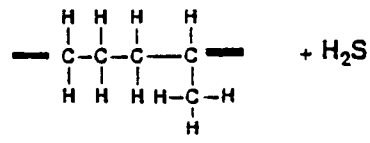

2-METHYLHEXANE

It should perhaps be emphasized that the interchain complexes on the right sides of reactions (10)–(14) should no more be regarded as static entities than inorganic complexes in aqueous electrolyte solutions or interfacial complexes sharing molecules on solid surfaces with those in aqueous solution. The stoichiometries of all such complexes simply correspond to idealized formulations representing the

statistical consequences of molecular interactions described by chemical reactions. The extent to which these reactions occur is controlled by the thermodynamic properties of the reactions and the activities of the species involved. It can be seen in reactions (10)–(14) that these include H_2O, H_2, O_2, NH_3, and H_2S. Use of these reactions to describe explicitly side chain interactions in proteins is analogous to the nearest-neighbor interaction approach adopted by Breslauer et al. [77], Turner et al. [78], and others to describe the thermodynamic behavior of DNA and RNA.

The side chain interactions represented by reactions (10)–(14) are rarely considered explicitly by protein chemists, who generally attribute the bulk of nearest-neighbor interactions in the cores of globular proteins to van der Waals forces and hydrogen bonds [79]. An alternative approach, and one perhaps more appropriate for describing the thermodynamic consequences of increasing temperature and pressure on protein folding, involves evaluating logarithmic analogs of the law of mass action for side chain interaction reactions, which in the case of reactions (10)–(14) can be written as

$$\frac{a_{\text{–Ethylisopropyl ester–}}\, a_{H_2O}}{a_{\text{–Aspartic acid}}\, a_{\text{Threonine–}}} = K_{(10)} \tag{15}$$

$$\frac{a_{\text{–4-Alkoxy-2-Hexanol–}}\, a_{H_2}}{a_{\text{–Serine}}\, a_{\text{Threonine–}}} = K_{(11)} \tag{16}$$

$$\frac{a_{\text{–Ethylaminopropyl ether–}}\, a_{O_2}^{1/2}}{a_{\text{–Asparagine}}\, a_{\text{serine–}}} = K_{(12)} \tag{17}$$

$$\frac{a_{\text{–Diethyl ester–}}\, a_{NH_3}}{a_{\text{–Asparagine}}\, a_{\text{serine–}}} = K_{(13)} \tag{18}$$

and

$$\frac{a_{\text{–Methylhexane–}}\, a_{H_2S}}{a_{\text{–Cysteine}}\, a_{\text{Isoleucine–}}} = K_{(14)} \tag{19}$$

respectively, where the letter a stands for the activity of the subscripted species in solution and $K_{(10)}$, $K_{(11)}$, $K_{(12)}$, $K_{(13)}$, and $K_{(14)}$ represent the equilibrium constants for the subscripted reactions. Research is currently under way in this laboratory to characterize such equilibrium constants as a function of temperature and pressure using a group contribution approach and the equations of state summarized in Appendix A. Application of these equations of state to calculation of the thermodynamic properties of aqueous biomolecules as a function of temperature and pressure is discussed briefly below.

5. Equations of state for aqueous biomolecules

The revised Helgeson, Kirkham, Flowers (HKF) [80] equations of state [81–83] summarized in Appendix A were developed originally to describe the temperature and pressure dependence of the thermodynamic properties of ionic and neutral

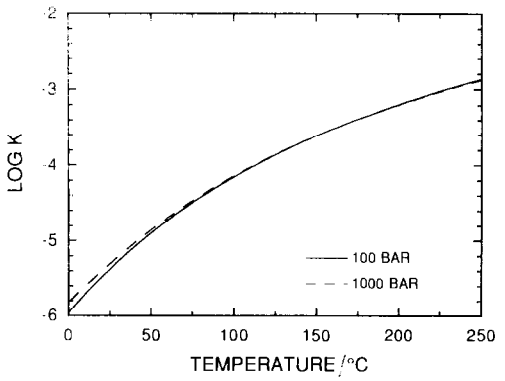

Fig. 11. Logarithm of the equilibrium constant for reaction (1) as a function of temperature at 100 and 1000 bar computed from $\log K = -\Delta\bar{G}_r^\circ/2.303RT$ using values of the standard partial molal Gibbs free energy of reaction ($\Delta\bar{G}_r^\circ$) generated with the aid of SUPCRT92 [83] using Eq. (A5) in Appendix A and equation of state parameters and thermodynamic data taken from Amend and Helgeson [90].

inorganic aqueous species [84,85], but they have since been applied to both charged and neutral organic aqueous species, including biomolecules at high temperatures and pressures [7,75,76,86–94]. An example is shown in Fig. 11, where the logarithm of the equilibrium constant for reaction (1) is plotted as a function of temperature at constant pressure. It can be deduced from this figure that reversible disproportionation of alanine to glycine and leucine is insensitive to increasing pressure, but strongly favored by increasing temperature. Nevertheless, if metastable equilibrium is maintained, alanine is favored over glycine and leucine at all the temperatures shown in the figure.

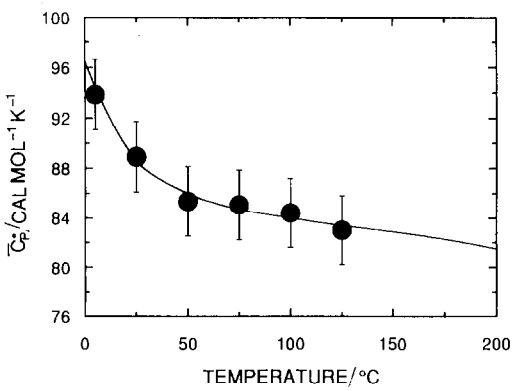

Fig. 12. Standard partial molal heat capacity ($\bar{C}_P^\circ$) of protonated butanamine as a function of temperature at P_{sat} (see the caption to Fig. 9). The symbols represent experimental data taken from Makhatadze and Privalov [96], but the curves were generated from Eq. (A2) in Appendix A with the aid of SUPCRT92 [83] using equations of state parameters computed from group contributions by regressing with Eq. (A2) a large data set of experimental standard partial molal heat capacities reported in the literature [91,92,94] (1 cal = 4.187 J).

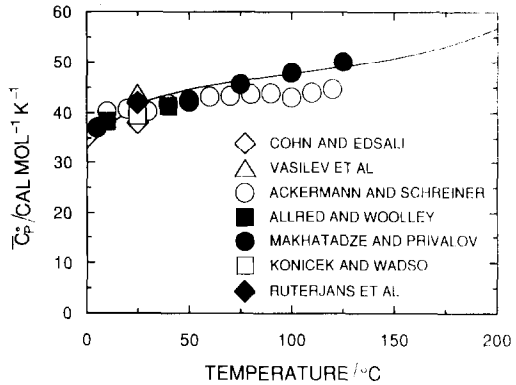

Fig. 13. Standard partial molal heat capacity ($\bar{C}_P^\circ$) of acetic acid as a function of temperature at P_{sat} (see the caption to Fig. 9). The symbols represent experimental data taken from the literature, but the curves were generated from Eq. (A2) in Appendix A with the aid of SUPCRT92 [83] using equations of state parameters computed from group contributions by regressing with Eq. (A2) a large data set of experimental standard partial molal heat capacities reported in the literature [91,92,94]. The sources of the data represented by the symbols in the legend correspond from top to bottom to references [96,116–121] (1 cal = 4.187 J).

Computed standard partial molal heat capacities ($\bar{C}_p^\circ$) of aqueous biomolecules at P_{sat} as a function of temperature can be compared with their experimental counterparts in Figs. 12 and 13, where it can be seen that the curves generated from Eq. (A2) in Appendix A are closely consistent with the experimental data represented by the symbols. Note in Fig. 12 that the curve representing $\bar{C}_p^\circ$ of protonated *n*-butanamine has a negative first derivative and exhibits a sigmoidal configuration with increasing temperature. In contrast, the curve for acetic acid in Fig. 13 has a positive first derivative and exhibits a reverse sigmoidal configuration with increasing temperature. Hence $\bar{C}_p^\circ$ of protonated *n*-butanamine decreases with increasing temperature, but that of acetic acid increases.

The standard partial molal thermodynamic properties of aqueous organic neutral molecules typically exhibit one of four types of behavior with increasing temperature and/or pressure [86,92,95]. Whether or not a given standard partial molal thermodynamic property of an aqueous species increases or decreases with increasing temperature at low temperature is a consequence of the effect of the aqueous species on the local solvent structure. In the case of nonaliphatic ionic species and strongly polar neutral molecules such as acetic acid, this effect is one of collapse of the solvent structure and solvation by H_2O dipoles, which results in decreasing $\bar{C}_p^\circ$ and $\bar{V}^\circ$ with decreasing temperature at low temperature. In contrast, the consequences of cavity formation in the solvent to accommodate charged and neutral aliphatic species at low temperatures depends on the property and the extent to which the effects of the structural disruption of the surrounding water dipoles by the molecule are offset by the effective charge or polarity of the species. For example, in the case of protonated *n*-butanamine in Fig. 12, the charged end of the

molecule causes local collapse of the solvent structure, but accommodation of the remainder of the molecule requires cavity formation, which for this molecule offsets the effect of the charge on the species and $\bar{C}_p^\circ$ consequently increases with decreasing temperature at low temperature. In the case of other aliphatic molecules such as protonated *n*-propylguanidine, the charge on the molecule dominates its calorimetric behavior and $\bar{C}_p^\circ$ values for this species maximize with increasing temperature [96]. In contrast, $\bar{C}_p^\circ$ values for nonpolar neutral aqueous species minimize with increasing temperature, but $\bar{V}^\circ$ for the same species may increase in a reverse sigmoidal fashion with increasing temperature. For example, in the case of a molecule such as aqueous ethylene (C_2H_2) the structural consequences of cavity formation cause $\bar{C}_p^\circ$ of this aqueous molecule to increase with decreasing temperature at low temperatures [97]. In contrast, $\bar{V}^\circ$ for aqueous C_2H_2 at low temperature decreases with decreasing temperature [98,99]. At high temperature, repulsion of H_2O dipoles and disruption of the electrostatic properties of the solvent in the vicinity of such neutral aqueous species cause both $\bar{C}_p^\circ$ and $\bar{V}^\circ$ of the species at P_{sat} in the liquid phase region (see the caption to Fig. 9) to increase with increasing temperature at high temperatures and approach infinity at the critical point of H_2O [85,97–102]. Electrolytes exhibit the opposite behavior [80,82,84,103–109]. In summary, depending on the thermodynamic property, some neutral aqueous species behave thermodynamically like electrolytes at low but not high temperature, and others behave thermodynamically like electrolytes at high but not low temperature. In other instances, the thermodynamic behavior of neutral aqueous species may resemble that of electrolytes at neither or both high and low temperature [95]. In cases such as protonated *n*-butanamine in Fig. 12, the thermodynamic properties of charged organic aqueous species may behave at low temperatures like those of nonpolar neutral aqueous species.

The standard partial molal heat capacities of the side chains of amino acids, peptides, and unfolded proteins also exhibit different types of behavior as a function of temperature, depending on their effective charge or polarity and the manner in which they affect the local solvent structure. For example, it can be seen in Fig. 14 that $\bar{C}_p^\circ$ for the side chain of aspartate ($-CH_2COO^-$) maximizes as a function of temperature, but that of the nonpolar side chain of phenylalanine ($-CH_2C_6H_5$) minimizes with increasing temperature. Although the side chain of tyrosine ($-CH_2C_6H_4OH$) is nominally polar, it is apparent in Fig. 14 that $\bar{C}_p^\circ$ for this molecule behaves like that of a nonpolar species and minimizes with increasing temperature. Although Privalov and Makhatadze [66,68] and Makhatadze and Privalov [67,96] attribute group contributions to the thermodynamic properties of proteins that decrease with increasing temperature to polar characteristics and those that increase with increasing temperature to nonpolar behavior, these distinctions take no account of the differential role of the solvent in determining the *effective* polarity of the side chains, which changes with increasing temperature. Note that the side chains of both asparagine ($-CH_2CONH_2$) and serine ($-CH_2OH$) are intrinsically polar, but it can be seen in Fig. 14 that $\bar{C}_p^\circ$ of the first of these increases with increasing temperature and that for $-CH_2OH$ decreases with increasing temperature. At high temperature, $\bar{C}_p^\circ$ for $-CH_2CONH_2$ behaves as though it were nonpolar, which is also true of $\bar{C}_p^\circ$ for $-CH_2OH$ at low temperature.

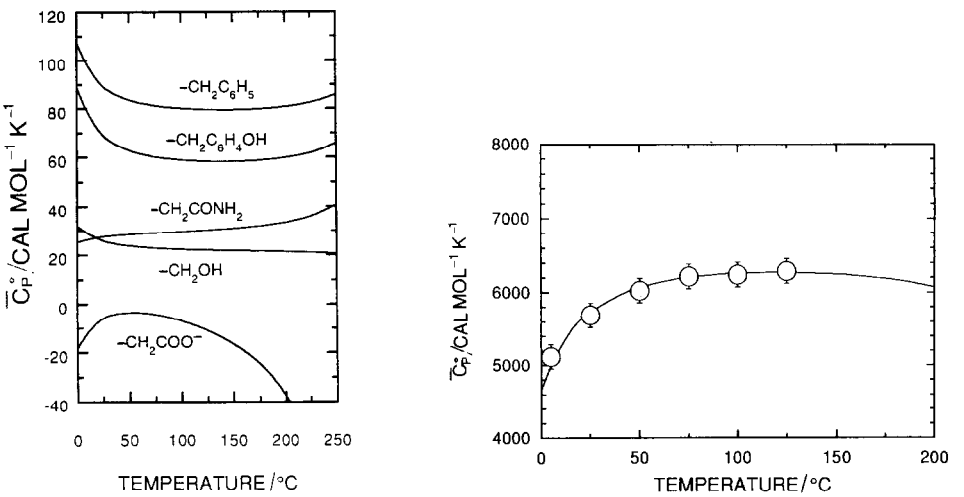

Fig. 14. Standard partial molal heat capacities of the side chains of phenylalanine ($-CH_2C_6H_5$), tyrosine ($-CH_2C_6H_4OH$), asparagine ($-CH_2CONH_2$), serine ($-CH_2OH$), and the aspartate anion ($-CH_2COO^-$) as a function of temperature at P_{sat} (see the caption to Fig. 9). The curves were generated from Eq. (A2) in Appendix A with the aid of SUPCRT92 [83] using equations of state parameters computed from group contributions by regressing with Eq. (A2) a large data set of experimental standard partial molal heat capacities reported in the literature [91,92,94]. (1 cal = 4.187 J).

Fig. 15. Standard partial molal heat capacity ($\bar{C}_P^*$) of unfolded cytochrome *c* as a function of temperature at P_{sat} (see the caption to Fig. 9). The symbols represent experimental data reported by Privalov and Makhatadze [68] for denatured cytochrome *c*, but the curves were generated from Eq. (A2) in Appendix A with the aid of SUPCRT92 [83] using equations of state parameters computed from group contributions by regressing with Eq. (A2) a large data set of experimental standard partial molal heat capacities reported in the literature [91,92,94]. (1 cal = 4.187 J).

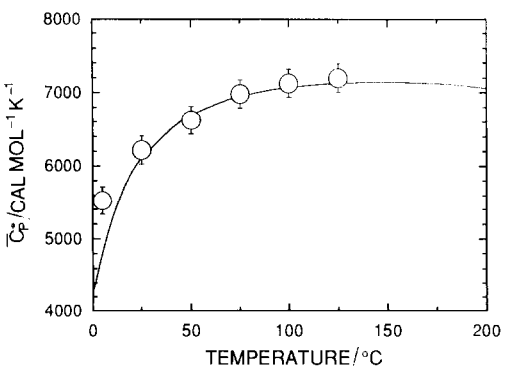

Fig. 16. Standard partial molal heat capacity ($\bar{C}_P^*$) of unfolded ribonuclease A as a function of temperature at P_{sat} (see the caption to Fig. 9). The symbols represent experimental data reported by Privalov and Makhatadze [68] for denatured ribonuclease A, but the curves were generated from Eq. (A2) in Appendix A with the aid of SUPCRT92 [83] using equations of state parameters computed from group contributions by regressing with Eq. (A2) a large data set of experimental standard partial molal heat capacities reported in the literature [91,92,94] (1 cal = 4.187 J).

It follows from the observations summarized in the preceding paragraph that curves representing the standard partial molal heat capacities of unfolded proteins as a function of temperature may in principle exhibit any one of the four dieffrent configurations shown in Fig. 14, depending on the number of each type of side chain that occurs in the amino acid sequence in the protein. Two examples are shown in Figs. 15 and 16, where it can be seen that the curves corresponding to computed values of $\bar{C}_p^\circ$ for both ribonuclease A and cytochrome *c* exhibit extrema. Although experimental data for denatured proteins are commonly extrapolated to higher temperatures assuming the heat capacities of proteins to be constant at high temperatures, it can be seen in Figs. 15 and 16 that the equations of state calculations represented by the curves indicate that $\bar{C}_p^\circ$ for unfolded ribonuclease A and cytochrome *c* maximize with increasing temperature at about 100 and at 150°C, respectively. Approximately 35% of the side chains in cytochrome *c* and about 24% of those in ribonuclease A are charged in the neutral pH range, which contributes substantially to the fact that $(\partial \bar{C}_p^\circ / \partial T)_{P_{sat}}$ for these proteins is negative at high temperature [92].

6. Concluding remarks

Although the equations of state summarized in Appendix A can be used to calculate the standard partial molal thermodynamic properties of aqueous biomolecules at elevated temperatures and pressures, a multitude of carefully controlled calorimetric and densimetric experiments will be needed before kinetic transition states and the thermodynamic behavior of these molecules can be characterized adequately at high temperatures and pressures. However, because aqueous biomolecules are so sensitive to their chemical environment at elevated temperatures and pressures, experimental measurements of their thermodynamic properties under these conditions cannot be interpreted unambiguously without controlling and/or monitoring the chemical potentials of H_2, CO_2, NH_3, and H_2S, as well as analyzing the aqueous phase for a spectrum of organic and inorganic molecules that may be produced by reactions of biomolecules with other aqueous species at elevated temperatures and pressures. The concentrations of many of these may not be quenchable, which will require at least some of the analyses to be done at high temperatures and pressures. To preclude artificially limiting reaction rates by slow rates of diffusional transfer in the absence of fluid flow in high temperature–pressure experiments, agitation and/or recirculation systems will have to be included in their design. The activation energies of chemical reactions among biomolecules and other aqueous species may be much higher than those of diffusion coefficients for aqueous organic species, which are generally of the order 3 kcal mol^{-1} [110]. In addition, Gibbs free energy minimization calculations should be carried out with the aid of equations of state to assist in interpreting calorimetric results and planning future experiments. Such computer calculations can be used together with analytical data to assess the degree to which metastable equilibrium states may have been established in hydrothermal experiments. They can also be

used to determine optimal activities of H_2, CO_2, HH_3, H_2S, and other species in solution to stabilize a given biochemical molecule or set of side chains over other related species at the temperature and pressure of interest. Constraining these activities in hydrothermal experiments should help ensure that the biochemical molecule of interest predominates in solution, and thus that calorimetric or solubility measurements represent the thermodynamic properties of the molecule and not a variant thereof. Such constraints are particularly important in high-temperature experimental studies of proteins and nucleic acids.

Although the chemical potentials of various components are routinely controlled in hydrothermal experiments involving minerals [111], the chemical potentials of H_2, CO_2, NH_3, H_2S, and other aqueous species are rarely constrained or even monitored in high-temperature/pressure experiments with biomolecules. However, without such constraints we will not be able to determine optimal conditions for growth of hyperthermobarophiles and carry out unambiguously critical measurements of the thermodynamic properties of proteins, nucleotides, nucleic acids, and other biochemical molecules at high temperatures and pressures. Although the challenge is formidable, the potential rewards of success are immeasurable. A vast new world of biochemical knowledge is waiting to be discovered at high temperatures and pressures which has implications and ramifications for both basic and applied medical science that go far beyond the paradigms of today.

Acknowledgments

The research described above was supported by the National Science Foundation (NSF grants EAR 77-14492, EAR 81-15859, EAR 8606052 and EAR 9117393), the Department of Energy (DOE contract DE-AT03-83ER-13100 and DOE grant DE-FG03-85ER-13419) and the Committee on Research at the University of California, Berkeley. We are indebted to Douglas Clark, John Baross, Jody Deming, Ken Dill, Peter Privalov, Robert Wood, and Everett Shock for helpful discussions during the course of this study. Thanks are also due Christine Owens, John Thompson, Rachel Walsh, and Alice Cheng for carrying out computer calculations, plotting, word processing, drafting, and photographic assistance. Finally, we express our appreciation to John Baross, Douglas Clark, Everett Shock, Vitalii Pokrovskii, Laurent Richard, and Christine Owens for their insightful and helpful reviews of the script.

References

[1] E.L. Shock, Orig. Life Evol. Biosph., 22 (1992) 67.
[2] E.L. Shock, Orig. Life Evol. Biosph., 22 (1992) 135.
[3] L.C. Price, Chem. Geol., 37 (1982) 215.
[4] L.C. Price, Geochim. Cosmochim. Acta, 57 (1993) 3261.
[5] E.L. Shock, Geochim. Cosmochim. Acta, 54 (1990) 1185.
[6] H.C. Helgeson, Geol. Soc. Am. Ann. Mtg. Abstr. Prog., 23 (1991) A25.

[7] H.C. Helgeson, A.M. Knox, C.E. Owens and E.L. Shock, Geochim. Cosmochim. Acta, 57 (1993) 3295.
[8] J.A. Baross and S.E. Hoffman, Origins Life, 15 (1985) 327.
[9] H.W. Jannasch and M.J. Mottl, Science, 229 (1985) 717.
[10] D.B. Hedrick, R.D. Pledger, D.C. White and J.A. Baross, FEMS Microbiol. Ecol., 101 (1992) 1.
[11] J.W. Deming and J.A. Baross, Geochim. Cosmochim. Acta, 57 (1993) 3219.
[12] J.A. Baross and J.W. Deming, in D.M. Karl (Ed.), The Microbiology of Deep Sea Hydrothermal Environments, CRC Press, Bocca Raton, FL, in press.
[13] K.O. Stetter, R. Huber, E. Blöchl, M. Kurr, R.D. Eden, M. Fielder, H. Cash and I. Vance, Nature, 365 (1993) 743.
[14] E.L. Shock, Geology, 16 (1988) 886.
[15] E.L. Shock, Geology, 17 (1989) 572.
[16] E.L. Shock, Orig. Life Evol. Biosph., 20 (1990) 331.
[17] A.H. Segerer, S. Burggraf, G. Fiala, G. Huber, R. Huber, U. Pley and K.O. Stetter, Orig. Life Evol. Biosph., 23 (1993) 77.
[18] J.A. Baross and J.W. Deming, Nature, 303 (1983) 423.
[19] D.S. Clark and R. Kelly, Chemtech, (1990) 654.
[20] R.J. Pledger, B.C. Crump and J.A. Baross, FEMS Microbiol. Ecol., in press.
[21] J.W. Schuliger, S.H. Brown, J.A. Baross and R.M. Kelly, Mol. Mar. Biol. Biotechnolog., 2 (1993) 76.
[22] M.W.W. Adams, Annu. Rev. Microbiol., 47 (1993) 627.
[23] R.Y. Morita and P.F. Mathemeier, J. Bacteriol., 88 (1964) 1667.
[24] P.C. Michels and D.S. Clark, in M.W.W. Adams and R.M. Kelly (Eds.), Biocatalysis at Extreme Temperatures: Enzyme Systems Near and Above 100°C, American Chemical Society, Washington, DC, 1992, p. 108.
[25] B. Zentgraf and T.J. Ahern, Pure Appl. Chem., 63 (1991) 1527.
[26] A. Zaks and A.M. Klibanov, Science, 224 (1984) 1249.
[27] E.J. Mathur, in M.W.W. Adams and R.M. Kelly (Eds.), Biocatalysis at Extreme Temperatures: Enzyme Systems Near and Above 100°C, American Chemical Society, Washington, DC, 1992, p. 189.
[28] K.O. Stetter, G. Fiala, G. Huber and A. Segerer, EMS Microbiol. Rev., 75 (1990) 117.
[29] R.H. White, Nature, 310 (1984) 430.
[30] G. Bernhardt, H.-D. Lüdemann, and R. Jaenicke, Naturwissenschaften, 71 (1984) 583.
[31] R.J.-C. Hennet, N.G. Holm and M.H. Engel, Naturwissenschaften, 79 (1992) 361.
[32] W.L. Marshall, Geochim. Cosmochim. Acta, 58 (1994) 2099.
[33] R. Hensel and H. König, FEMS Microbiol. Lett., 49 (1988) 75.
[34] D.R. Musgrave, K.M. Sandman, D. Stroup and J.N. Reeve, in M.W.W. Adams and R.M. Kelly (Eds.), Biocatalysis at Extreme Temperatures: Enzyme Systems Near and Above 100°C, American Chemical Society, Washington, DC, 1992, p. 174.
[35] R. Huber, M. Kurr, H.W. Jannasch and K.O. Stetter, Nature, 342 (1989) 833.
[36] M. Kurr, R. Huber, H. König, H.W. Jannasch, H. Fricke, A. Trincone, J.K. Kristjansson and K.O. Stetter, Arch. Microbiol., 156 (1991) 239.
[37] G. Fiala and K.O. Stetter, Arch. Microbiol., 145 (1986) 56.
[38] W.J. Jones, J.A. Leigh, F. Mayer, C.R. Woese and R.S. Wolfe, Arch. Microbiol., 136 (1983) 254.
[39] R.J. Pledger and J.A. Baross, J. Gen. Microbiol., 137 (1991) 203.
[40] G. Erauso, A.-L. Reysenbach, A. Godfroy, J.-R. Meunier, B. Crump, F. Partensky, J.A. Baross, V. Marteinsson, G. Barbier, N.R. Pace and D. Prieur, Arch. Microbiol., 160 (1993) 338.
[41] J.F. Miller, E.L. Almond, N.N. Shah, J.M. Ludlow, J.A. Zollweg, W.B. Streett, S.H. Zinder and D.S. Clark, Biotechnol. Bioeng., 31 (1988) 407.
[42] C.M. Nelson, M.R. Schuppenhauer and D.S. Clark, Appl. Environ. Microbiol., 58 (1992) 1789.
[43] S.L. Miller and J.L. Bada, Nature, 334 (1968) 609.

[44] J.L. Bada, Phil. Trans. R. Soc. London, Ser. B, 333 (1991) 349.
[45] J.L. Bada, M. Zhao and S.L. Miller, Geol. Soc. Am. Ann. Mtg. Abstr. Prog., 23 (1991) A25.
[46] J.L. Bada, S.L. Miller and M. Zhao, Orig. Life Evol. Biosph., in press.
[47] J.D. Trent, R.A. Chastain and A.A. Yayanos, Nature, 307 (1984) 737.
[48] J.A. Baross and J.W. Deming, Nature, 307 (1984) 740.
[49] J.A. Baross, J.W. Deming and R.R. Becker, in M.J. Klug and C.A. Reddy (Eds.), Current Perspectives in Microbial Ecology: Third International Symposium on Microbial Ecology, American Society for Microbiology, Washington, DC, 1984, p. 186.
[50] J.A. Baross, personal communication, 1993.
[51] J.B. Corliss, J.A. Baross and S.E. Hoffman, Ocean. Acta, 4 (1981) 56.
[52] N. Kishima and H. Sakai, Geochem. J., 18 (1984) 19.
[53] H. Yanagawa and K. Kobayashi, Orig. Life Evol. Biosph., 22 (1992) 147.
[54] N. Kishima, Geochim. Cosmochim. Acta, 53 (1989) 2143.
[55] H.L. Barnes, in G.C. Ulmer and H.L. Barnes (Eds.), Hydrothermal Experimental Techniques, Wiley, New York, 1987, p. 507.
[56] T.S. Bowers and H.C. Helgeson, Geochim. Cosmochim. Acta, 47 (1983) 1247.
[57] A.B. Belonoshko, P. Shi and S.K. Saxena, Comp. Geosci., 18 (1992) 1267.
[58] S.W. Fox and C.R. Windsor, Science, 170 (1970) 984.
[59] B.M. French, Ph.D. Dissertation, The Johns Hopkins University, Baltimore, MD, 1964.
[60] D.E. Ingmanson and M.J. Dowler, Orig. Life Evol. Biosph., 8 (1977) 221.
[61] D.J. Ingle, Persp. Biol. Med., 15 (1972) 254.
[62] P.L. Privalov, Adv. Protein. Chem., 33 (1979) 167.
[63] P.L. Privalov, Annu. Rev. Biophys. Chem., 18 (1989) 47.
[64] P.L. Privalov, Thermochim. Acta, 163 (1990) 33.
[65] P.L. Privalov and S.L. Gill, Adv. Protein. Chem., 39 (1988) 191.
[66] P.L. Privalov and G.I. Makhatadze, J. Mol. Biol., 232 (1993) 660.
[67] G.I. Makhatadze and P.L. Privalov, J. Mol. Biol. (1993) 639.
[68] P.L. Privalov and G.I. Makhatadze, J. Mol. Biol., 213 (1990) 385.
[69] G.I. Makhatadze, V.N. Medvedkin and P.L. Privalov, Biopolymers, 30 (1990) 1001.
[70] H.R. Constantino, S.H. Brown and R.M. Kelly, J. Bacteriol., 172 (1990) 3654.
[71] J.F. Miller, C.M. Nelson, J.M. Ludlow, N.N. Shah and D.S. Clark, Biotechnol. Bioeng., 34 (1989) 1015.
[72] D.J. Hei and D.S. Clark, Appl. Environ. Microbiol., 60 (1994) 932.
[73] S. Burggraf, H. Fricke, A. Neuner, J. Kristjansson, P. Rouvier, L. Mandelco, C.R. Woese and K.O. Stetter, System. Appl. Microbiol., 13 (1990) 263.
[74] J.P. Amend and H.C. Helgeson, Geol. Soc. Am. Ann. Mtg. Abstr. Prog., 23 (1991) A212.
[75] E.L. Shock, Geol. Soc. Am. Ann. Mtg. Abstr. Prog., 22 (1990) A158.
[76] E.L. Shock, Geochim. Cosmochim. Acta, 57 (1993) 3341.
[77] K.J. Breslauer, R. Frank, H. Blocker and L.A. Marky, Proc. Natl. Acad. Sci. USA, 83 (1986) 3746.
[78] D.H. Turner and N. Sugimoto, Annu. Rev. Biophys. Chem., 17 (1988) 167.
[79] K.A. Dill, Biochemistry, 29 (1990) 7133.
[80] H.C. Helgeson, D.H. Kirkham and G.C. Flowers, Am. J. Sci., 281 (1981) 1249.
[81] J.C. Tanger IV and H.C. Helgeson, Am. J. Sci., 288 (1988) 19.
[82] E.L. Shock, E.H. Oelkers, J.W. Johnson, D.A. Sverjensky and H.C. Helgeson, J. Chem. Soc. Faraday Trans., 88 (1992) 803.
[83] J.W. Johnson, E.H. Oelkers and H.C. Helgeson, Comp. Geosci., 18 (1992) 899.
[84] E.L. Shock and H.C. Helgeson, Geochim. Cosmochim. Acta, 52 (1988) 2009.
[85] E.L. Shock, H.C. Helgeson and D.A. Sverjensky, Geochim. Cosmochim. Acta, 53 (1989) 2157.
[86] E.L. Shock and H.C. Helgeson, Geochim. Cosmochim. Acta, 54 (1990) 915.
[87] E.L. Shock, in M. Lewan and E. Pittman (Eds.), The Role of Organic Acids in Geological Processes, Springer-Verlag, New York.
[88] E.L. Shock, Am. J. Sci., 294 (1994).

[89] H.C. Helgeson, Appl. Geochem., 7 (1992) 291.
[90] M.D. Schulte and E.L. Shock, Geochim. Cosmochim. Acta, 57 (1993) 3835.
[91] J.P. Amend and H.C. Helgeson, in preparation.
[92] J.P. Amend and H.C. Helgeson, in preparation.
[93] J.P. Amend and H.C. Helgeson, in preparation.
[94] J.P. Amend, H.C. Helgeson and E.L. Shock, in preparation.
[95] H.C. Helgeson, Geochim. Cosmochim. Acta (Robert M. Garrels Memorial Issue) 56 (1992) 3197.
[96] G.I. Makhatadze and P.L. Privalov, J. Mol. Biol., 213 (1990) 375.
[97] D.R. Biggerstaff, Ph.D Dissertation, University of Delaware, 1986.
[98] D.R. Biggerstaff and R.H. Wood, J. Phys. Chem., 92 (1988) 1994.
[99] D.R. Biggerstaff and R.H. Wood, J. Phys. Chem., 92 (1988) 1988.
[100] D.R. Biggerstaff, D.E. White and R.H. Wood, J. Phys. Chem., 89 (1985) 4378.
[101] R. Crovetto, R.H. Wood and V. Majer, J. Chem. Thermodyn., 22 (1990) 231.
[102] R. Crovetto, R.H. Wood and V. Majer, J. Chem. Thermodyn., 23 (1991) 1139.
[103] V. Majer, J.A. Gates, A. Inglese and R.H. Wood, J. Chem. Thermodyn., 20 (1988) 949.
[104] V. Majer, A. Inglese and R.H. Wood, J. Chem. Thermodyn., 21 (1989) 321.
[105] V. Majer, A. Inglese and R.H. Wood, J. Chem. Thermodyn., 21 (1989) 397.
[106] V. Majer, R. Crovetto and R.H. Wood, J. Chem. Thermodyn., 23 (1991) 333.
[107] V. Majer, L. Hui, R. Crovetto and R.H. Wood, J. Chem. Thermodyn., 23 (1991) 213.
[108] D.E. White, R.H. Wood and D.R. Biggerstaff, J. Chem. Thermodyn., 20 (1988) 159.
[109] R.H. Wood, R.W. Carter, J.R. Quint, V. Majer, P.T. Thompson and J.R. Boccio, J. Chem. Thermodyn., 26 (1994) 225.
[110] E.H. Oelkers, Geochim. Cosmochim. Acta, 55 (1991) 3515.
[111] G.C. Ulmer and H.L. Barnes (Eds.), Hydrothermal Experimental Techniques, Wiley, New York, 1987.
[112] D.A. Sverjensky, E.L. Shock and H.C. Helgeson, in preparation.
[113] G. Lauerer, J.K. Kristjansson, T.A. Langworthy, H. König and K.O. Stetter, System. Appl. Microbiol., 8 (1986) 100.
[114] K.O. Stetter, H. König and E. Stackebrandt, System. Appl. Microbiol., 4 (1983) 535.
[115] D.S. Clark, personal communication, 1993.
[116] E.J. Cohn and J.T. Edsall (Eds.), Proteins, Amino Acids and Peptides as Ions and Dipolar Ions, Reinhold, New York, 1943.
[117] V.A. Vasilev, E.Y. Shevehenko, N.V. Fedyainov and M.V. Golikov, Iavanovo, Khimiko tekhnologicheske fi Institut, 20 (1977) 1557.
[118] T. Ackermann and F. Schreiner, Z. Elektrochem., 62 (1958) 1143.
[119] G.C. Allred and E.M. Wooley, J. Chem. Thermodyn., 13 (1981) 155.
[120] J. Konicek and I. Wadsö, Acta Chem. Scand., 25 (1971) 1541.
[121] H. Rüterjans, F. Schreiner, U. Sage and T. Ackermann, J. Phys. Chem., 73 (1969) 986.

Appendix A: equations of state

The revised Helgeson, Kirkham, Flowers (HKF) [80] equations of state [81,84–86] can be used to calculate the thermodynamic properties of organic and inorganic charged and neutral aqueous species at elevated temperatures and pressures. These equations of state are given by

$$\Delta\bar{V}^{\circ} = a_1 + \frac{a_2}{\Psi + P} + \left(a_3 + \frac{a_4}{\Psi + P}\right)\left(\frac{1}{T - \Theta}\right) - \omega Q + \left(\frac{1}{\varepsilon} - 1\right)\left(\frac{\partial \omega}{\partial P}\right)_T \qquad \text{(A1)}$$

$$\bar{C}_p^\circ = c_1 + \frac{c_2}{(T-\Theta)^2} - \left(\frac{2T}{(T-\Theta)^3}\right)\left(a_3(P-P_r) + a_4 \ln\left(\frac{\Psi+P}{\Psi+P_r}\right)\right) + \omega T X + 2TY\left(\frac{\partial\omega}{\partial T}\right)_P - T\left(\frac{1}{\varepsilon}-1\right)\left(\frac{\partial^2\omega}{\partial T^2}\right)_P \quad \text{(A2)}$$

$$\bar{S}^\circ = \bar{S}^\circ_{P_r,T_r} + c_1 \ln\left(\frac{T}{T_r}\right) - \frac{c_2}{\Theta}\left[\left(\frac{1}{T-\Theta}\right) - \left(\frac{1}{T_r-\Theta}\right) + \frac{1}{\Theta}\ln\left(\frac{T_r(T-\Theta)}{T(T_r-\Theta)}\right)\right] + \left(\frac{1}{T_r-\Theta}\right)^2\left(a_3(P-P_r) + a_4\ln\left(\frac{\Psi+P}{\Psi+P_r}\right)\right) - \omega Y - \left(\frac{1}{\varepsilon}-1\right)\left(\frac{\partial\omega}{\partial T}\right)_P - \omega_{P_r,T_r} Y_{P_r,T_r} \quad \text{(A3)}$$

$$\Delta\bar{H}^\circ \equiv \Delta\bar{H}_f^\circ + (\bar{H}^\circ_{P,T} - \bar{H}^\circ_{P_r,T_r}) = \Delta\bar{H}_f^\circ + c_1(T-T_r) - c_2\left(\left(\frac{1}{T-\Theta}\right) - \left(\frac{1}{T_r-\Theta}\right)\right) + a_1(P-P_r) + a_2\ln\left(\frac{\Psi+P}{\Psi+P_r}\right) + \left(\frac{2T-\Theta}{(T-\Theta)^2}\right) \times \left(a_3(P-P_r) + a_4\ln\left(\frac{\Psi+P}{\Psi+P_r}\right)\right) + \omega\left(\frac{1}{\varepsilon}-1\right) + \omega T Y - T\left(\frac{1}{\varepsilon}-1\right)\left(\frac{\partial\omega}{\partial T}\right)_P - \omega_{P_r,T_r}\left(\frac{1}{\varepsilon_{P_r,T_r}}-1\right) - \omega_{P_r,T_r} T_r Y_{P_r,T_r} \quad \text{(A4)}$$

and

$$\Delta\bar{G}^\circ \equiv \Delta\bar{G}_f^\circ + (\bar{G}^\circ_{P,T} - \bar{G}^\circ_{P_r,T_r}) = \Delta\bar{G}_f^\circ - \bar{S}^\circ_{P_r,T_r}(T-T_r) - c_1\left(T\ln\left(\frac{T}{T_r}\right) - T + T_r\right) + a_1(P-P_r) + a_2\ln\left(\frac{\Psi+P}{\Psi+P_r}\right) - c_2\left[\left(\left(\frac{1}{T-\Theta}\right) - \left(\frac{1}{T_r-\Theta}\right)\right)\left(\frac{\Theta-T}{\Theta}\right) - \frac{T}{\Theta^2}\ln\left(\frac{T_r(T-\Theta)}{T(T_r-\Theta)}\right)\right] + \left(\frac{1}{T-\Theta}\right)\left(a_3(P-P_r) + a_4\ln\left(\frac{\Psi+P}{\Psi+P_r}\right)\right) + \omega\left(\frac{1}{\varepsilon}-1\right) - \omega_{P_r,T_r}\left(\frac{1}{\varepsilon_{P_r,T_r}}-1\right) + \omega_{P_r,T_r} X_{P_r,T_r}(T-T_r) \quad \text{(A5)}$$

where $\bar{V}^\circ$, $\bar{C}_p^\circ$, and $\bar{S}^\circ$ represent the standard partial molal volume, heat capacity, and entropy of the species at P and T; $\Delta\bar{H}^\circ$ and $\Delta\bar{G}^\circ$ refer to the apparent standard partial molal enthalpy and Gibbs free energy of formation of the species at P and T; a_1, a_2, a_3, a_4, c_1, and c_2 stand for temperature/pressure-independent parameters for the species; T_r, P_r, T, and P designate the reference temperature of 298.15 K, the reference pressure of 1 bar, and the temperature and pressure of interest, respectively; $\Delta\bar{H}_f^\circ$ and $\Delta\bar{G}_f^\circ$ denote the standard partial molal enthalpy

and Gibbs free energy of formation from the elements in their stable form at P_r and T_r; $(\bar{H}^{\circ}_{P,T} - \bar{H}^{\circ}_{P_r,T_r})$ and $(\bar{G}^{\circ}_{P,T} - \bar{G}^{\circ}_{P_r,T_r})$ correspond to the difference in the conventional standard partial molal enthalpy and Gibbs free energy of an aqueous species at P and T and those at P_r, T_r; ε stands for the dielectric constant of H_2O; Ψ and Θ refer to solvent parameters equal to 2600 bar and 228 K, respectively; Q, X, and Y represent Born functions given by

$$Q \equiv \frac{1}{\varepsilon}\left(\frac{\partial \ln \varepsilon}{\partial P}\right)_T \tag{A6}$$

$$X \equiv \frac{1}{\varepsilon}\left(\left(\frac{\partial^2 \ln \varepsilon}{\partial T^2}\right)_P - \left(\frac{\partial \ln \varepsilon}{\partial T}\right)^2_P\right) \tag{A7}$$

$$Y \equiv \frac{1}{\varepsilon}\left(\frac{\partial \ln \varepsilon}{\partial T}\right)_P \tag{A8}$$

and ω stands for the conventional Born coefficient of the species, which can be expressed as

$$\omega = \frac{166027 Z_e^2}{r_e} - 53870Z \tag{A9}$$

where Z_e and Z stand for the effective and formal charge (which are equivalent for charged species), respectively, and r_e denotes the effective electrostatic radius of the species, which for monatomic ions is given by

$$r_e = r_x + |Z|(k_Z + g) \tag{A10}$$

where r_x designates the crystal radius of the ion; $k_Z = 0.0$ for anions and 0.94 for cations; and g stands for a solvent function of density and temperature given by Shock et al. [82]. If the species under consideration has no formal charge, $(\partial\omega/\partial P)_T$, $(\partial\omega/\partial T)_P$, and $(\partial^2\omega/\partial T^2)_P$ in Eqs. (A1)–(A4) are taken to be zero [85]. In the absence of crystal radii and experimental data at high temperatures and pressures, values of a_1, a_2, a_3, a_4, c_1, c_2, and ω_{P_r,T_r} in Eqs. (A3)–(A5) can be estimated for both charged and neutral aqueous species using algorithms given by Shock and Helgeson [75,84–87,89,91–94,112].

Equations (A1)–(A8) have been incorporated in a computer program called SUPCRT92 [83] which includes data files for about 500 minerals, gases, and aqueous charged and neutral inorganic and organic species. The code can be obtained at no cost from the Laboratory of Theoretical Geochemistry (otherwise known as Prediction Central) in the Department of Geology and Geophysics at the University of California, Berkeley. The SUPCRT92 software package is in the process of being revised and updated to include many more organic aqueous species, as well as equations of state for organic solids, liquids, and gases.